

Proceeding Paper

Optimal Load Shedding Scheme Considering the Dynamic Frequency Response [†]

Carlos Lozada ^{1,*}, Walter Vargas ², Nelson Granda ² and Marlon Chamba ¹

¹ Operador Nacional de Electricidad (CENACE), Quito 17211991, Ecuador; mchamba@cenace.gob.ec

² Department of Electrical Engineering, Faculty of Electrical and Electronic Engineering, Campus José Rubén Orellana Ricaurte, Escuela Politécnica Nacional, Quito 170525, Ecuador; walter.vargas@epn.edu.ec (W.V.); nelson.granda@epn.edu.ec (N.G.)

* Correspondence: clozada@cenace.gob.ec

[†] Presented at the XXXII Conference on Electrical and Electronic Engineering, Quito, Ecuador, 13–15 November 2024.

Abstract: A power system is never in a steady state due to continuous load variations, disturbances, maneuvers, and the operation of protection systems. A generation deficit causes a frequency drop in the system that must be controlled. If this frequency deviation is not properly managed, it can result in the loss of synchronism between generators and, eventually, lead to a partial or even total system collapse. This article presents a load shedding scheme applied to the IEEE 39-bus New England system. The scheme considers an N-1 contingency space to evaluate the dynamic frequency response, aiming to determine the appropriate settings for low-frequency relays activated by the rate of change of frequency (ROCOF).

Keywords: load shedding; optimal load shedding scheme; dynamic frequency response; rate of change of frequency; ROCOF

1. Introduction

Power system stability is defined as the ability of a power system to remain in an operational equilibrium state under normal operating conditions and to evolve to an acceptable equilibrium state after a disturbance [1]. A power system can be vulnerable to instability problems when operating near its physical limits; these problems must be controlled, or they can lead to partial or even total system collapse. Traditionally, the following types of stabilities exist: angular stability, voltage stability, and frequency stability.

Frequency stability is associated with the balance between power generation and electrical demand. When there is a variation in power generation, it causes a deviation in the system frequency, which can result in values outside the safe operating ranges. To maintain stability, power–frequency controllers are incorporated to regulate the balance between generation and demand, ensuring that the frequency remains within appropriate operating ranges [2].

Power–frequency control can be organized into three levels: primary, secondary, and tertiary. The main characteristics of each control level are their specific operational time ranges and associated variables. Primary control aims to limit the frequency deviation during a contingency, restoring the balance between power generation and electrical demand by bringing the system to a new operating point where the frequency differs from the nominal value. This control operates within a time range of 2 to 30 s. The primary frequency response results from the interaction of generator inertia, load damping, speed regulators, and other devices that supply energy to the system, such as battery energy storage systems (BESSs) [3].



Citation: Lozada, C.; Vargas, W.; Granda, N.; Chamba, M. Optimal Load Shedding Scheme Considering the Dynamic Frequency Response. *Eng. Proc.* **2024**, *77*, 25. <https://doi.org/10.3390/engproc2024077025>

Academic Editor: Jaime Cepeda

Published: 18 November 2024



Copyright: © 2024 by the authors. Licensee MDPI, Basel, Switzerland. This article is an open access article distributed under the terms and conditions of the Creative Commons Attribution (CC BY) license (<https://creativecommons.org/licenses/by/4.0/>).

Secondary control operates in a time range of 30 s to 10 min. It operates within the control area, considering the frequency and power exchange with neighboring areas, and it is implemented by Automatic Generation Control (AGC). Finally, tertiary control operates in a time margin greater than 10 min. It acts in the scope of a large electrical system, seeking optimized load sharing to ensure sufficient energy reserves [3]. During the operation of the EPS, situations may arise in which imbalances between generated power and consumed power are significantly pronounced. In these circumstances, the mechanical valves controlled by the governors may be too slow to react in time before the frequency crosses acceptable operating limits. This may violate safe operating parameters, which could result in damage to the generating units [1,4]. In these cases, remedial strategies consisting of under-frequency load shedding or generation tripping are designed to prevent possible damage to the generating machines and the collapse of the system.

Load shedding strategies can be classified into the following categories: conventional, computational, and adaptive [5]. These categories identify the value of frequency and *ROCOF* for the operation of their algorithms. Strategies involving *ROCOF* have been investigated to achieve better results by identifying the minimal amount of load that needs to be disconnected in critical scenarios.

Reference [6] proposes a scheme that estimates the rate of change of frequency (*ROCOF*) at the center of inertia (CoI) and, consequently, the size of the generation loss using local frequency measurements. An innovative turning point detection technique is presented to eliminate the effect of local frequency oscillations.

Reference [7] presents a methodology based on time-domain simulations to obtain the frequency evolution in response to generation loss across various operating scenarios. These scenarios are classified based on the rate of change of frequency (*ROCOF*). A prioritized list of loads for disconnection is generated. Using these results, a load shedding scheme is proposed, and its performance is compared through dynamic simulations.

Reference [8] proposes sizing the storage capacity for virtual energy contribution based on *ROCOF*. In this article, *ROCOF* measurements are identified locally, and calculations are performed using center of inertia parameters. This technique is applied to specific areas of the system; however, it does not provide a characterization of the system under different contingencies.

Reference [9] describes a methodology for identifying characteristic *ROCOFs* (rate of change of frequency) in a power system under N-1 contingencies. This methodology is applied to the IEEE 39-bus New England system to determine the number of *ROCOFs* that may arise during dynamic frequency behavior. Based on these results, appropriate load shedding measures can be established.

2. Methodology

The rate of change of frequency (*ROCOF*) is a critical indicator of the robustness of an electrical power system. Analyzing the dynamic behavior of this parameter enables the estimation of power imbalances within the system, which can be calculated using the following equation.

$$ROCOF = \frac{\Delta P}{S} \cdot \frac{f}{2H} \quad (1)$$

where ΔP represents the power imbalance caused by an event, f denotes the nominal frequency of the EPS, H is the system's total inertia constant after the event, and S refers to the system's nominal power [10]. The *ROCOF* calculation, as part of the proposed methodology, is performed using a 0.5-s window, following the recommendations provided in [11–13].

The proposed methodology employs a reduced first-order model to represent the system's frequency response. This model facilitates the calculation of the dynamic frequency response to an imbalance between generation and load, providing an effective tool for stability analysis. Comprising a turbine, a speed governor, a synchronous generator, and a

load, the model allows for a more efficient evaluation of the influence of these elements on frequency stability. The process flow of the methodology is illustrated in Figure 1.



Figure 1. Stages of the proposed methodology.

2.1. Representative Events of the Contingency Space

An equivalent first-order model is implemented to characterize the dynamic frequency response using the following variables: load imbalance (ΔP_o), system control regulation (R), and load damping (D). It is assumed that the dynamic capacity available is a fraction (F) of the immediate reserve capacity, while the complementary fraction ($1 - F$) is represented as a first-order lag with a time constant (T). Additionally, (K_m) is a gain constant for the spinning reserve of the generators. The proposed model considering N generators is illustrated in Figure 2 [14].

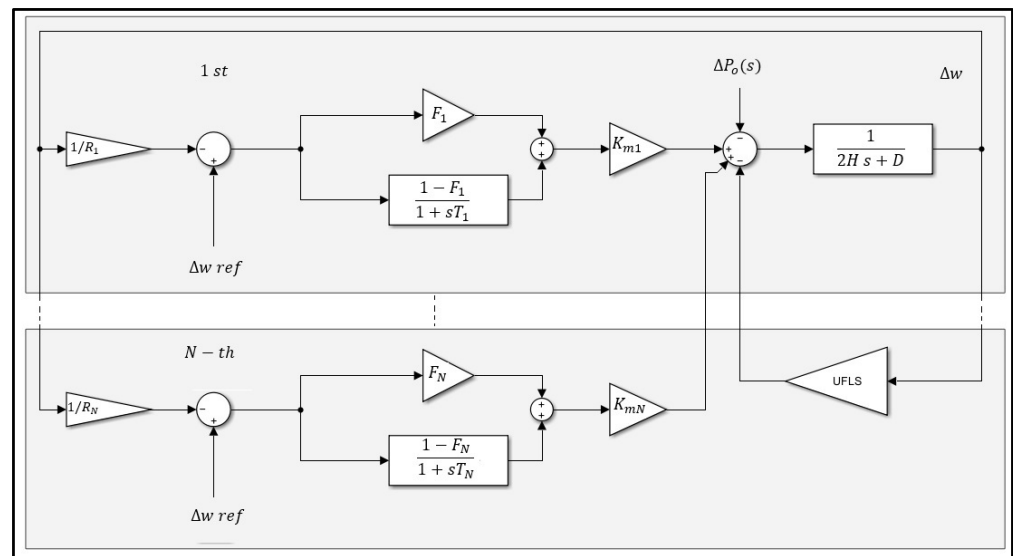


Figure 2. First-order model for dynamic frequency response.

Reference [9] details the methodology used to develop a first-order model for the dynamic frequency response. Monte Carlo simulations are used to generate possible operational scenarios, which are then subjected to $N - 1$ contingencies to evaluate their behavior. Subsequently, a database is created that includes parameters such as the rate of change of frequency ($ROCOF$), the system’s equivalent inertia before and after the contingency, the generation loss power during the event, and the NADIR. Using this database, an unsupervised classification algorithm known as Clustering is applied. The results obtained with this methodology are shown in Table 1 and Figure 3.

Table 1. Representative events of the contingency space.

Groups	ROCOF [Hz/s]	Hpre	Hpos	Pout	NADIR
Cluster 1	−0.38	4.89	4.57	403.75	58.72
Cluster 2	−0.30	4.89	4.63	322.99	59.08
Cluster 3	−0.25	4.88	4.66	270.70	59.31

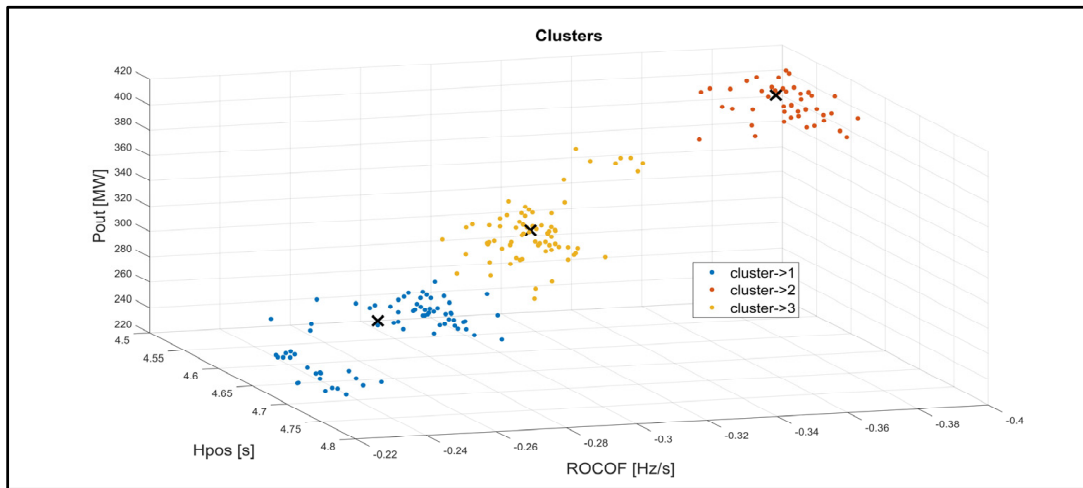


Figure 3. Correlation of variables *ROCOF*, *Hpos*, and *Pout*.

2.2. Optimization

After identifying the events that represent the behavior of the established database, load shedding optimization is performed using the “surrogateopt” algorithm available in MATLAB 2021a. This algorithm aims to minimize the percentage of load shed, with the objective function specifically designed to achieve this minimization.

2.2.1. Mathematical Modeling of the Optimization Problem

Problem definition:

$$FO : \min \left\{ \sum_{i=1}^n C_i(\Delta t_i) \times P_{load_i} \right\} \quad (2)$$

where i : representative scenario; P_{load_i} : system demand in scenario i ; Δt_i : variation in relay actuation time and measurement; $C_i(\Delta t_i)$: percentage of load shed; n : number of representative scenarios.

Decision Variables:

$$C_i(\Delta t_i) : \text{Percentage of load shed.} \quad (3)$$

Constraints:

$$F_{ss_i} > 59.2 \text{ Hz} \quad (4)$$

$$t_{i+1} - t_i < 5 \text{ ms} \quad (5)$$

$$0 < C_i < 1 \quad (6)$$

where F_{ss} : Stabilization Frequency; t_i : Action Time of Scenario i .

ROCOF calculation is performed using a 0.5 s time window. The database must be restructured by excluding scenarios where the system returns to safe levels after a contingency. The selection criterion is based on the *NADIR*: scenarios in which the frequency does not drop below the 59.4 Hz threshold are considered safe and removed from the database. The 59.4 Hz value corresponds to the first stage of under-frequency load shedding, as recommended in [15].

2.2.2. Definition of *ROCOF* Settings for Relays

As a result of implementing the previous stages, the *ROCOF* values for the centroids of each characteristic group within the system’s $N - 1$ contingency universe are obtained and denoted by the symbol x in Figure 3.

These values provide statistical insights into potential events within the system. For the optimization model, it is assumed that the *ROCOF* threshold required to activate the protection relay has already been identified.

In this context, the frequency derivative value for each centroid must be adjusted to cover the associated cluster elements. To achieve this, the risk management criterion based on the mean and standard deviation proposed in [16] is used. Figure 4 illustrates the effect of this adjustment; the solid black lines represent the mean of the *ROCOF* values for the associated group; the dashed lines represent the standard deviation of the *ROCOF* values for the associated group; the colored solid lines represent the *ROCOF* set for each associated group. Additionally, the statistical analysis for the *ROCOF* values of group 3 (blue) is shown in the box.

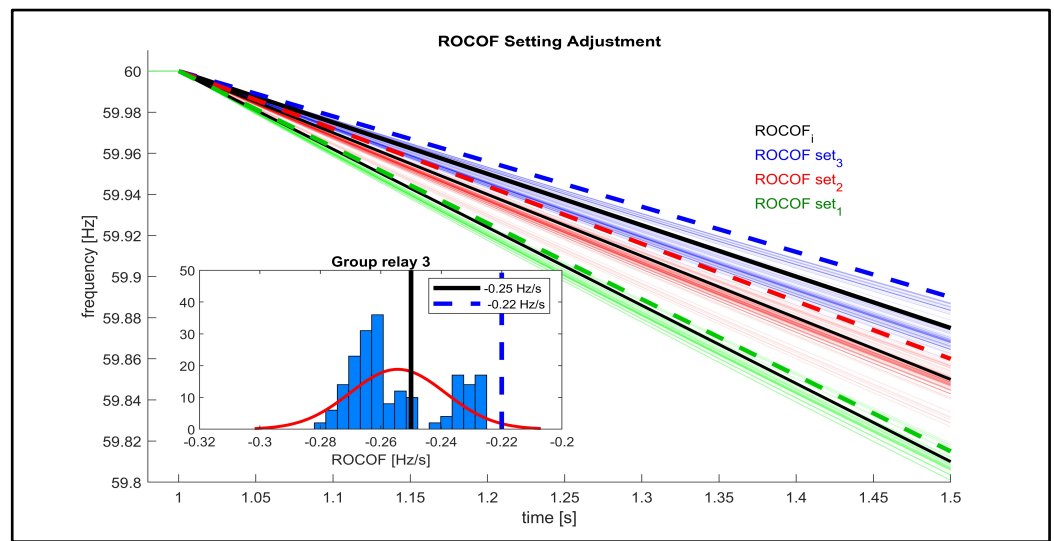


Figure 4. ROCOF setting adjustment.

Criterion Based on the Mean and Standard Deviation:

$$ROCOF_{set} = u - 2\sigma \tag{7}$$

where $ROCOF_{set}$: the variable considered for optimization; u : the mean of the *ROCOF* values for the associated group; and σ : the standard deviation of the *ROCOF* values for the associated group.

For the implementation of the heuristic optimization algorithm, the stochastic variation of the percentage of load that must be disconnected based on the demand at that moment is considered. The frequency behavior is evaluated for each of the defined *ROCOF* settings, given that three distinct settings must be coordinated to ensure the selectivity of the protections.

In this context, a model of a *ROCOF*-activated low-frequency protection relay is implemented for each characteristic group. The objective is to have a stochastic parameter that determines the delay time each relay must consider before sending the trip signal, thereby ensuring the selectivity of the protection settings.

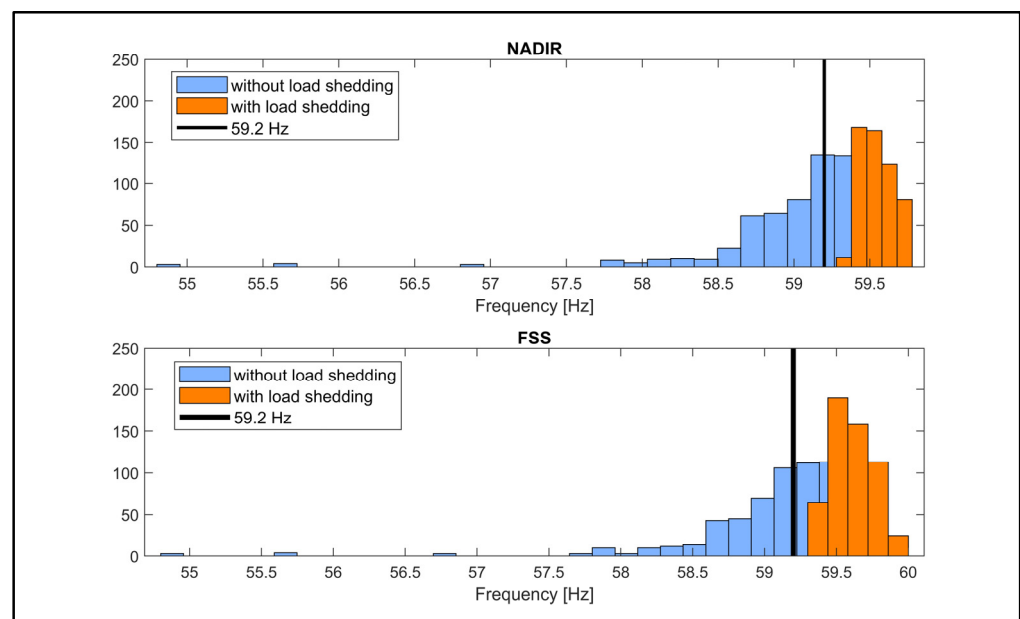
3. Application of the Methodology and Analysis of Results

The test system used is an IEEE 39 bus bar system. This system has nineteen loads, ten generators, twelve transformers, and thirty-five transmission lines, whose data can be found in reference [17]. In the present study, a specific modification was made that involves dividing the original generators into eighteen to increase the sensitivity in the analysis of N-1 contingency events. After applying the proposed methodology, the results are presented in Table 2.

Table 2. Settings of each low-frequency relay based on representative groups.

Groups	ROCOF Set [Hz/s]	Load Shed [%]	Delay Δt [s]
Relay 1	−0.37	5.8	0.21
Relay 2	−0.28	2.2	0.51
Relay 3	−0.22	1.1	0.84

To evaluate the methodology, all scenarios generated in the MCS were analyzed by placing the protection relays with the obtained settings. Figure 5 shows a histogram comparing the stabilization frequency (*FSS*) values and the lowest frequency point (*NADIR*) before and after implementing the protection relays. This comparison demonstrates a shift towards safer frequency values, thereby validating the implemented methodology.

**Figure 5.** Comparison histograms of the methodology's impact on frequency.

4. Conclusions and Recommendations

The application of the present methodology assumes that the speed regulators are functioning correctly and that there is an accurate identification of machine variables such as machine inertia, power limits, and regulator droop, among others explained in the methodology. Therefore, a preliminary parameter validation stage must be conducted before applying this methodology.

The present methodology has the characteristic of observing different conditions of the electrical system as long as the input variables, such as generation loss power, *ROCOF*, and post-contingency equivalent inertia, are identified. These variables can be easily obtained by reading the current state of the system. This characteristic justifies its application in systems with a high penetration of non-inertial and low-inertia generation, such as photovoltaic and wind power plants, and even considering synthetic inertia responses provided by batteries.

In the present methodology, equivalents of the generator-governor groups were implemented to simplify the analysis. These equivalents can be used to perform a zonal analysis in systems with large generation parks. This requires a preliminary analysis to identify zones with very similar frequency behavior. However, for a more detailed analysis, it is recommended to use the entire network, although this would require significantly higher computational capacity.

Author Contributions: Methodology, software, and investigation: C.L.; Conceptualization: W.V.; Project administration: N.G.; Supervision, review, and editing: M.C. All authors have read and agreed to the published version of the manuscript.

Funding: This research received no external funding.

Institutional Review Board Statement: Not applicable.

Informed Consent Statement: Not applicable.

Data Availability Statement: Data are contained within the article.

Conflicts of Interest: The authors declare no conflicts of interest.

Abbreviations

ROCOF	Rate of Change of Frequency
EPS	Electric Power System
UFLS	Under Frequency Load Shedding
Governors	Speed Regulators
BESS	Battery Energy Storage System
NADIR	Lowest Point of the Frequency
AGC	Automatic Generation Control
MCS	Monte Carlo Simulation
Hpre	Equivalent Inertia before the Contingency
Hpos	Equivalent Inertia after the Contingency
Pout	Lost Generation Power
ΔP_o	Load Power Variation
$\Delta \omega$	Speed Variation
$Km_i, F_i, T_i,$ and R_i	Meters of the First-Order Reduced Model
H_{eq}	Equivalent System Inertia
D	Load Damping

References

- Kundur, P.; Balu, N.J. *Power System Stability and Control*; McGraw-Hill: New York, NY, USA, 1994; ISBN 978-0-7803-3463-2.
- Vargas, W.; Chamba, S.; Torre, A.D.L.; Echeverría, D. Protocolo de pruebas y validación de reguladores de velocidad—Aplicación práctica en la central hidroeléctrica Delsitanisagua. *Rev. Téc. Energ.* **2022**, *19*, 22–33. [[CrossRef](#)]
- Chamba, S.; Vargas, W.; Echeverría, D.; Riofrio, J. Regulación Primaria de Frecuencia Mediante Sistemas de Almacenamiento de Energía con Baterías en el Sistema Eléctrico Ecuatoriano. *Rev. Téc. Energ.* **2022**, *19*, 13–21. [[CrossRef](#)]
- Rudez, U.; Mihalic, R. Analysis of Underfrequency Load Shedding Using a Frequency Gradient. *IEEE Trans. Power Deliv.* **2011**, *26*, 565–575. [[CrossRef](#)]
- Laghari, J.A.; Mokhlis, H.; Bakar, A.H.A.; Mohamad, H. Application of Computational Intelligence Techniques for Load Shedding in Power Systems: A Review. *Energy Convers. Manag.* **2013**, *75*, 130–140. [[CrossRef](#)]
- Sun, M.; Liu, G.; Popov, M.; Terzija, V.; Azizi, S. Underfrequency Load Shedding Using Locally Estimated ROCOF of the Center of Inertia. *IEEE Trans. Power Syst.* **2021**, *36*, 4212–4222. [[CrossRef](#)]
- Granda, N.; Jácome, V. Esquema Automático de Alivio de Carga para Sistemas Eléctricos que sirven a Plataformas Petroleras. *Rev. Téc. Energ.* **2023**, *19*, 58–68. [[CrossRef](#)]
- Alonso Sørensen, D.; Vázquez Pombo, D.; Torres Iglesias, E. Energy Storage Sizing for Virtual Inertia Contribution Based on ROCOF and Local Frequency Dynamics. *Energy Strategy Rev.* **2023**, *47*, 101094. [[CrossRef](#)]
- Lozada, C.X.; Vargas, W.A.; Granda, N.V.; Chamba, M.S. Methodology for Identifying Representative Rates of Change of Frequency (ROCOFs) in an Electric Power System against N-1 Contingencies. *Eng. Proc.* **2023**, *47*, 8. [[CrossRef](#)]
- Egido, I.; Fernandez-Bernal, F.; Centeno, P.; Rouco, L. Maximum Frequency Deviation Calculation in Small Isolated Power Systems. *IEEE Trans. Power Syst.* **2009**, *24*, 1731–1738. [[CrossRef](#)]
- Wu, L. Power System Frequency Measurement Based Data Analytics and Situational Awareness. Ph.D. Thesis, University of Tennessee, Knoxville, TN, USA, 2018.
- Wright, P.S.; Davis, P.N.; Johnstone, K.; Rietveld, G.; Roscoe, A.J. Field Measurement of Frequency and ROCOF in the Presence of Phase Steps. *IEEE Trans. Instrum. Meas.* **2019**, *68*, 1688–1695. [[CrossRef](#)]
- ENTSOE. *Rate of Change of Frequency (ROCOF) Withstand Capability: ENTSO-E Guidance Document for National Implementation for Network Codes on Grid Connection*; ENTSO-E: Brussels, Belgium, 2017.
- Aik, D.L.H. A General-Order System Frequency Response Model Incorporating Load Shedding: Analytic Modeling and Applications. *IEEE Trans. Power Syst.* **2006**, *21*, 709–717. [[CrossRef](#)]

15. Centro Nacional de Control de Energía. *Determinación Del Esquema De Alivio De Carga Por Baja Frecuencia Para El Sistema Nacional Interconectado*; CENACE: Quito, Ecuador, 2022.
16. Chamba, M.; Vargas, W.; Cepeda, J. Evaluación probabilística de la estabilidad transitoria considerando la incertidumbre de la demanda y gestión del riesgo. *Rev. Téc. Energ.* **2018**, *15*, 1–10. [[CrossRef](#)]
17. Athay, T.; Podmore, R.; Virmani, S. A Practical Method for the Direct Analysis of Transient Stability. *IEEE Trans. Power Appar. Syst.* **1979**, *PAS-98*, 573–584. [[CrossRef](#)]

Disclaimer/Publisher’s Note: The statements, opinions and data contained in all publications are solely those of the individual author(s) and contributor(s) and not of MDPI and/or the editor(s). MDPI and/or the editor(s) disclaim responsibility for any injury to people or property resulting from any ideas, methods, instructions or products referred to in the content.